RESEARCH ARTICLE

Raman Characterization of Single-Walled Nanotubes of Various Diameters Obtained by Catalytic Disproportionation of CO

J. E. Herrera, L. Balzano, F. Pompeo, and D. E. Resasco*

School of Chemical Engineering and Materials Science, University of Oklahoma, Norman, Oklahoma, USA

Single-walled carbon nanotubes prepared by disproportionation of CO over Co-Mo/SiO_2 catalysts have been characterized by Raman spectroscopy, using several excitation energies. By varying the reaction temperature, different ranges of nanotube diameter were obtained. The average diameter of a single-walled nanotube produced at 750 °C was 0.9 nm, while it increased up to about 1.5 nm when the synthesis was conducted at 950 °C. The analysis of the Raman spectra obtained with a range of laser excitation energies not only gives a definite description of the single-walled nanotubes diameters but also helps differentiate the metallic or semiconducting character of the samples. This analysis can be done by comparing the experimental data with calculated gap energies as a function of nanotube diameter as well as comparing the relative intensity of bands centered at 50–60 cm^{-1} lower than the tangential *G* mode. The analysis of this feature, which can be fitted with a Breit–Wigner–Fano line, offers a method for distinguishing between metallic and semiconducting single-walled carbon nanotubes.

Keywords:

1. INTRODUCTION

Since their discovery, single-walled carbon nanotubes (SWNTs) have opened a research field of great interest due to their potential applications in nanostructured materials and nanoscale devices.[1] Indeed, they exhibit exceptional chemical and physical properties that have unlocked a vast number of possibilities.[2] The procedures most commonly used for SWNT production include arc discharge, laser ablation, and catalytic decomposition of carbon-containing compounds over a metal catalyst.[3,4] This catalytic decomposition method has attracted much attention because it appears to be promising technique for scaling-up the production process at a relatively low cost. Not only may this type of process operate under conditions that are less energy-intensive than other methods[5,6] but also it can lead to a controlled growth of SWNT by varying operating parameters such as temperature, catalyst, reaction gas, etc.[7,8]

The control of the structural properties is an attractive prospect given that the diameter and chirality of a SWNT determine its electronic structure. However, scientists have not yet been able to produce significant amounts of homogeneous SWNT material with specific physical properties. The catalytic decomposition (sometimes referred to as chemical vapor deposition) of a carbon-containing molecule on low-surface-area samples, such as a catalytically patterned surface or over isolated metal nanoparticles, has been proposed as an approach to diameter control.[9] However, these methods would not be amenable to the development of a continuous process and they would not be suitable for large-scale operations. The use of small metal particles dispersed on a high-surface-area support opens the possibility of producing large amounts of SWNT, using continuous processes that are similar to conventional catalytic processes, such as ethylene polymerization. Some reports have indicated that synthesis of nanotube samples with varying diameter distributions is possible with the catalytic method by using different types of metal catalysts[10] or by changing the working temperature. For instance, Peigney et al.[8] using an Fe-alumina catalyst for the synthesis of SWNTs by CH_4 decomposition, found different diameter distributions as the reaction temperature varied. However, low selectivities to SWNTs were achieved in that study. Together with SWNT, the product showed a substantial amount of double- and triple-walled carbon nanotubes. In another recent study[6] no trend in the diameter of the SWNT produced at different temperatures was found from CH_4 decomposition over a Fe–Mo alumina supported catalyst.

*Author to whom correspondence should be addressed.

  1533-4880/2003/01/001/006/$17.00+.25 doi:10.1166/jnn.2003.153

However, in this case, the selectivity to SWNTs was also low and any trend may have been masked by the presence of other carbon formations.

Clearly, without an effective tailoring of the catalyst formulation, the variation in temperature by itself cannot ensure control of both SWNT selectivity and specific diameter. In a previous investigation,[11] we combined the use of a highly selective catalyst with changes in synthesis temperature to systematically vary the diameter distribution of the SWNT. Our highly selective catalyst is based on Co-Mo/SiO_2 with low Co/Mo ratio, and it shows its best performance under the disproportionation of CO in the temperature range 700–950 °C.[12] We found that, as the synthesis temperature is increased, there is a clear increase in the average SWNT diameter and a broadening in the diameter distribution. We have explained this temperature dependence of the SWNT diameter in terms of the morphology changes that occur on the catalyst as the reaction proceeds. On a selective Co–Mo catalyst, most Co is in the form of a surface layer of cobalt molybdate over highly dispersed particles of Mo oxide. As the CO disproportionation starts, Mo oxide is converted into Mo carbide. This transformation breaks up the Co molybdate layer, allowing for the reduction of Co by CO. The resulting Co clusters are highly dispersed and in the presence of a high concentration of CO in the gas phase. This environment is favorable for the production of a SWNT, whose diameter is determined by the size of the Co clusters. Therefore, as the reaction temperature increases, the rate of Co agglomeration becomes higher; therefore, the nanotubes are formed from larger Co clusters, thus resulting in larger SWNT diameters. It is interesting to note that similar increases in tube diameter have been observed when the ambient temperature is raised in vapor phase techniques such as arc discharge and laser ablation, in which a higher temperature should not necessarily lead to larger metal particle sizes. For example, Bandow et al.[13] found a similar increase in tube diameter with temperature working with pulsed laser vaporization of a heated, metal-catalyzed, carbon target in Ar gas. They observed that the average tube diameter went from 1.0 to about 1.2 nm when the ambient temperature was raised from 780 to 1000 °C. Similar results have been obtained by Rinzler et al.[14] and by Yudasaka et al.[15] in laser ablation systems. Although the results are similar the causes for the increase of nanotube diameter with temperature are significantly different. That is, in the case of vaporized metals (arc discharge and laser ablation), the time needed for the metal to cool to a temperature at which the solubility limit is exceeded obviously increases with the ambient temperature. During this time, the metals agglomerate and then the "embryo" is formed at a larger size than when the ambient temperature is lower. In the case of SWNT growth catalyzed on a solid surface, the increase in temperature accelerates sintering of the clusters, so the "embryo" configuration occurs at a larger size, thus resulting in larger diameter.

The characterization of the SWNT obtained in the previous contribution was done by transmission electron microscopy (TEM) and Raman spectroscopy, but only using one excitation energy. Although the results of Raman and TEM were in excellent agreement, the information resulting from the Raman analysis with only one laser energy does not represent the whole range of nanotube diameters. Since the Raman intensity is strongly affected by resonance phenomena, the radial breathing mode peaks obtained at each laser energy do not reflect the entire diameter distribution of the sample but rather the subset of nanotubes that are in resonance with the laser photons. Therefore, in order to get information that is more representative of the diameter distribution of the SWNTs in the sample, it is necessary to probe the SWNT with several excitation energies. Due to the resonance phenomena, Raman spectroscopy can be used to probe both structural and electronic features of the nanotubes.[16] The Raman spectra of SWNTs exhibit several important bands: (a) a radial A_{1g} breathing mode, whose position can be used to calculate the nanotube diameter[17] (accurate estimates can only be obtained if intertube coupling is considered, since a significant upshift of the radial breathing mode (RBM) is observed for nanotubes in bundles with respect to isolated nanotubes[18]); (b) the so-called *D*-band at around 1350 cm^{-1}, which is related to disordered carbon and the presence of carbon nanoparticles and amorphous carbon;[19] (c) a tangential mode *G* band appearing in the 1400–1700 cm^{-1} region, which is related to the Raman-allowed phonon mode E_{2g}. The analysis of the tangential band offers a method for distinguishing between metallic and semiconducting single-walled carbon nanotubes, since peak broadening and extra bands centered at around 1540 cm^{-1} are clearly seen when metallic nanotubes are present in the sample. The origin of this extra feature, which can be fitted with a Breit–Wigner–Fano line, is the resonance of the incident or scattered laser photon with the lowest optical transition (E_{11}) between the one-dimensional density of states singularities in the valence and conduction bands of metallic SWNTs.[7, 20]

In this contribution, we have expanded our previous work and have verified the dependence of the Raman resonance of the metallic modes on the diameter distribution of the samples studied. The results obtained for the tangential modes are compared with results obtained for the breathing mode of the SWNTs under study and with the theoretical predictions of the metallic or semiconducting nature of the different nanotubes that are probed at each laser energy. This analysis provides further evidence of our ability to vary the nanotube diameter by controlling the catalyst formulation and operating temperatures.

2. EXPERIMENTAL DETAILS

A silica-supported Co–Mo bimetallic catalyst was prepared using cobalt nitrate and ammonium heptamolybdate salts as precursors. The SiO_2 support obtained from Aldrich had an average pore size of 6 nm, BET area 480 m^2/g, pore volume 0.75 cm^3/g, and particle sizes in the range 70–230 mesh. The total metallic loading in the catalyst was 2 wt% while the Co:Mo molar ratio was 1:3. Prior to the production of SWNT by CO disproportionation, the catalyst was heated in H_2 flow to 500 °C, and then in He flow to the reaction temperature. It has been shown[5] that this reduction/heating pretreatment is essential to obtain a high selectivity to SWNTs. The CO disproportionation reaction used for the production of SWNTs was conducted in a fixed bed catalytic reactor at a temperature that varied from 700 to 950 °C in flow of pure CO at a total pressure of 5 atm. Following reaction, a sequence of treatments was carried out in order to separate the SWNT from the catalyst. The first step in this sequence was a low-temperature oxidation for the elimination of the amorphous carbon, which was accomplished by calcination in air at 300 °C for 2 h. The second step was the removal of the silica support. In this step, 1 g of the material was suspended in a NaOH 0.2 M solution, while stirring for 24 h at 65 °C. After filtering through a Teflon-PTFE 0.2 mm membrane, the remaining solid was washed with deionized water until the pH was neutral. Then, the solid was dried overnight at room temperature inside a desiccator. The third step was the elimination of the metals (Co and Mo). This was accomplished by an oxidative attack in wet air for 24 hours at 300 °C followed by sonication on HCl 6 M for 10 minutes. Again, the solid part was filtered and washed, as before. The total removal of silica and metals after both steps was greater than 90%, as determined by temperature-programmed oxidation of the carbon in the sample.

The TEM images were obtained in a JEOL JEM-2000FX electron microscope. For this analysis, a suspension in isopropanol was achieved by stirring the solid sample with ultrasound for 10 min. A few drops of the resulting suspension were deposited on a TEM grid and subsequently dried and evacuated before the analysis. The Raman spectra were obtained in a Jovin Yvon-Horiba Lab Ram equipped with a charge coupled device detector and with three different laser excitation sources having wavelengths of 632 (He–Ne laser), 514, and 2.55 eV (Ar laser).

3. RESULTS AND DISCUSSION

Figure 1 shows a typical micrograph obtained by TEM on a sample obtained by CO disproportionation at 850 °C on a Co–Mo (1:3)/SiO_2 catalyst after 2 h reaction. Bundles of SWNTs are clearly observed together with some residual metallic particles. Two types of metallic particles are

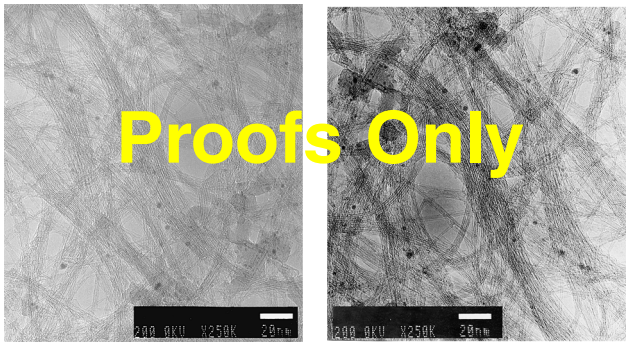

Fig. 1. Typical TEM micrograph of a SWNT produced by CO disproportionation at 850 °C on a Co:Mo catalyst during 2 h. The carbon yield on this sample is 30 g C per g Co, and the selectivity to SWNT is higher than 90%.

observed, relatively large particles, which have no participation in the synthesis of the SWNT and small clusters of about the same size as the SWNT, which we believe are responsible for the formation of the SWNT.

We have previously reported that the diameter distribution of SWNT obtained by this method strongly depends on the reaction temperature. Specifically, we found that the average diameter for the SWNT obtained at a reaction temperature of 750 °C was around 0.9 nm, for those obtained at 850 °C it was 1.2 nm, and for samples obtained at 950 °C it was 1.5 nm.[11] These results correlated very well with the distribution of nanotube diameters inferred from the analysis of the A_{1g} RBM frequency in the Raman spectra.[17]

As mentioned above, the Raman spectrum of a SWNT results from a resonant process associated with optical transitions in the one-dimensional electronic density of states, which fall in the visible and near infrared range.[16, 21] Moreover, the energy of the allowed optical transitions depends on both the diameter and the metallic or semiconductor character of the nanotubes.[22, 23] Consequently, when the excitation energy is close to that of an allowed optical transition, the Raman intensity is greatly enhanced. Therefore, by employing different excitation energies different nanotubes can be probed.

Figure 2 shows the breathing mode range in the Raman spectra obtained with three different laser excitation energies on SWNT samples obtained at different temperatures. It can be seen that the spectra for a given sample are quite different, depending on the laser excitation energy used, but the same trend is observed at all energies. That is, the bands clearly shift to lower wavenumbers as the reaction temperature increases. Since the frequency of the radial breathing mode is inversely proportional to the nanotube diameter,[24] this shift indicates an increase in diameter as temperature increases, in excellent agreement with our previous report.[11]

Linking nanotube diameters with the energy gaps between singularities in the valence and conduction bands

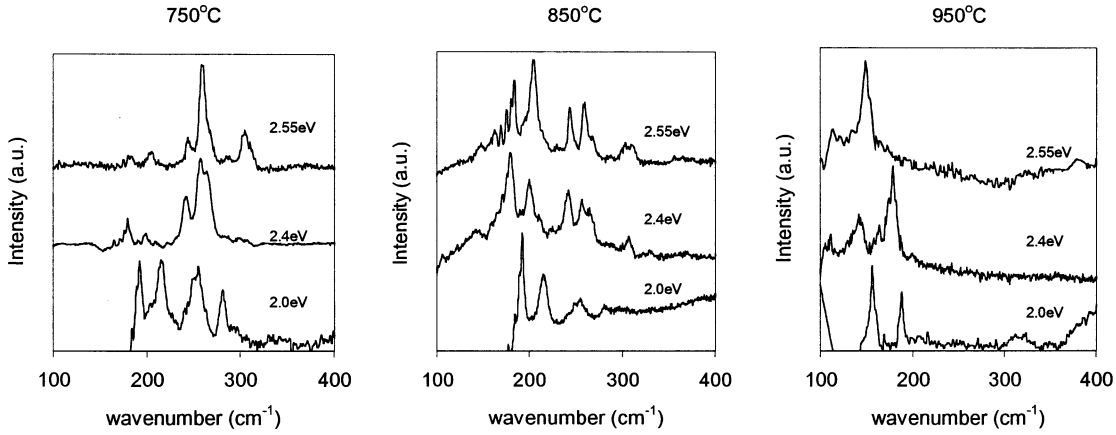

Fig. 2. Radial breathing mode resonant Raman spectra of SWNT grown for 2 hours in pure CO at the indicated temperatures on a Co:Mo catalyst. The excitation wavelengths were 488 (2.55 eV), 514 (2.4 eV), and 633 nm (2.0 eV).

of the electronic density of states of SWNTs is possible by calculating the one-dimensional energy band structure of SWNTs. These calculations have been conducted by Kataura et al.[22] and their results are reproduced in Figure 3 and compared to our experimental data. In this figure, the calculated results for each individual nanotube were used as a background, with the solid and open circles represent nanotubes with metallic and semiconducting character, respectively. Superimposed over this background, the Raman data obtained in the present work are indicated with solid diamonds. Points are marked for the particular energy of the laser employed (i.e., 2.0, 2.4, or 2.55 eV) and for each observed nanotube diameter, as inferred from the frequency of the radial breathing mode bands.

The TEM observations for the SWNT sample obtained at 750 °C indicated an average nanotube diameter of 0.9 nm.[11] Consequently, a "metallic window" can be delineated around this average diameter, for which the resonance condition for metallic nanotubes would take place in the energy region 2.4–2.7 eV. Therefore, it is expected that, for this diameter range, the two lasers with higher energy (2.4 and 2.55 eV), which fall within this window would only probe metallic nanotubes. By inspecting Figure 3a, one can see that, in agreement with this expectation, the RBM bands detected with the two lasers of higher energy correspond to metallic SWNTs only. By contrast, with the lower energy laser (2.0 eV) we probe both semiconducting and metallic nanotubes. In fact, since the TEM observations indicated that the

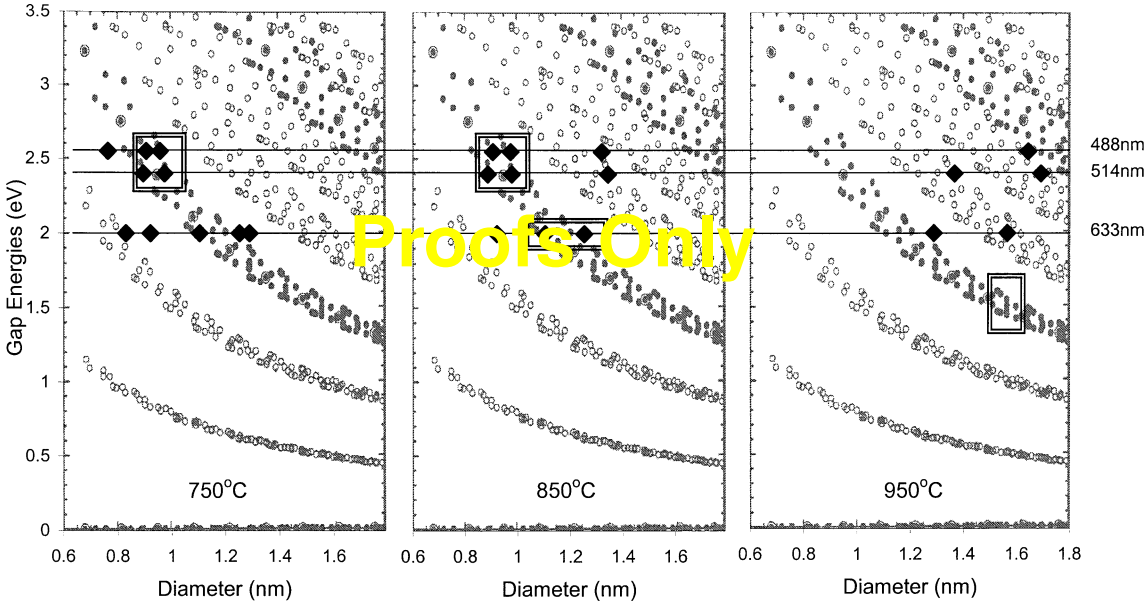

Fig. 3. Background: Calculated gap energies as a function of diameter for SWNT with chiral indexes with larger diameter than (5,5) as a function of diameter. (Adapted with permission from [18], A. M. Rao et al., *Phys. Rev. Lett.* 86, 3895 **(2001)**. © 2001, Elsevier Science.) Superimposed data: The solid diamonds indicate the diameter of the SWNTs as determined from the radial breathing mode bands of the Raman spectra of the samples obtained at the indicated temperatures (750, 850, and 950 °C) with the three different laser energies 488 (2.55 eV), 514 (2.4 eV), and 633 nm (2.0 eV).

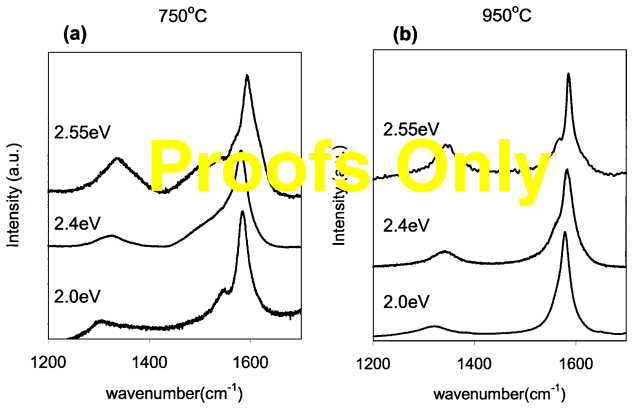

Fig. 4. Raman spectra in the tangential mode (*G* band) region obtained with three different laser excitation energies, for SWNT samples produced by CO disproportionation at 750 (a) and 950 °C (b).

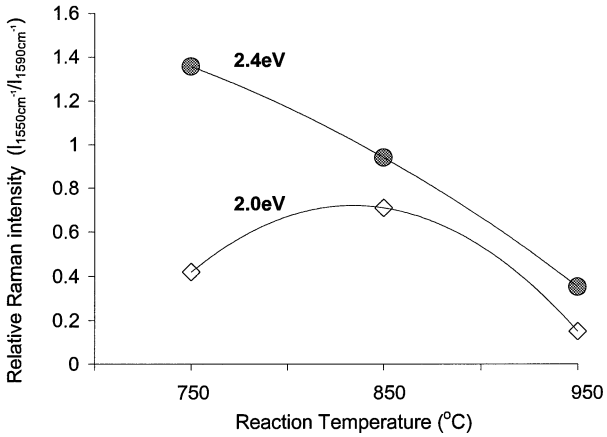

Fig. 5. Raman excitation profiles calculated from the relative Raman intensity of the modes associated with metallic nanotubes in the tangential mode (*G* band) obtained with laser excitation energies of 2.4 and 2.0 eV for SWNT samples produced by CO disproportionation at 750, 850, and 950 °C.

majority of the nanotubes in this sample had diameters around 0.9 nm, the bands observed at frequencies corresponding to larger diameters and with metallic character should represent only a small fraction of the sample.

In good correspondence with these data, the high frequency Raman spectra of Figure 4a, corresponding to the sample synthesized at 750 °C, displays a clear difference between the features seen at each laser energy. With the laser excitations of 2.55 and 2.4 eV, a broad and asymmetric Raman peak was observed to the left of the *G* band, which clearly demonstrates the presence of metallic nanotubes in resonance with the laser excitation energy. However, for the 2.0 eV laser, the left shoulder was much smaller. Pimenta et al.[16] have also investigated the variation of the band attributed to metallic nanotubes and described by the Breit–Wigner–Fano line shape centered at 1540 cm^{-1} as a function of the laser energy. However, in that particular study the large enhancement in the 1540/1593 cm^{-1} intensity ratio was observed at lower laser energies than those at which we observe the enhancement. The position of the "metallic window" was shifted, because the nanotubes they used had diameters in the 1.1–1.3 nm range. As can be predicted from the plot in Figure 3, for those diameters the energy region of resonance for metallic nanotubes falls in the range 1.7–2.2 eV, which agrees very well with the range at which they observed enhancement of the 1540/1593 cm^{-1} intensity ratio. A similar conclusion was reached by Kataura et al.[22] for SWNTs obtained by arc discharge using a RhPd catalyst. In this particular case, most of the SWNTs produced had diameters distributed from 0.7 to 1.0 nm and consequently when using laser energies around 1.8 eV mostly metallic SWNTs were probed.

We can expand the same analysis to interpret the data obtained on the samples synthesized at higher temperatures. For instance, Figure 4b shows the high frequency Raman spectra obtained using three different laser energies on the nanotubes produced at 950 °C. In this case, the contribution of the 1540 cm^{-1} band to the overall spectra is less significant for all three different excitation energies than on the sample synthesized at 750 °C. As seen in Figure 3, the "metallic window" for a sample with an average diameter of 1.5 nm should occur at laser energies below 1.6 eV. Then, all of the observed bands at laser energies above 2.0 eV correspond to semiconducting nanotubes. In good agreement with this analysis, the Raman spectra did not show the characteristic resonance that is described by the Breit–Wigner–Fano line.

Another interesting trend is illustrated in Figure 5; in this case, we plot the ratio of the area under the 1540 cm^{-1} feature to that of the 1593 cm^{-1} main *G* band of the Raman spectra obtained with two different excitation energies, for nanotubes grown at three different temperatures. The results obtained at 2.0 and 2.4 eV show a remarkable contrast. First, it can be seen that the ratio for the SWNTs probed with the 2.4 eV laser greatly decreased as the reaction temperature increased. This can be interpreted in terms of the gap energy plots as a function of nanotube diameter shown in Figure 3. As the reaction temperature increased, nanotubes of larger diameters were formed and, at this particular laser energy, the fraction of semiconducting nanotubes probed by Raman increased. In consequence, of all the SWNTs formed at 750 °C, only the metallic ones were probed at 2.4 eV, while of all those formed at 950 °C, only the semiconducting nanotubes were probed.

The results obtained with the 2.0 eV excitation energy clearly confirm the previous trend. In this case, the maximum contribution of modes characteristic to metallic nanotubes occurred for the SWNT grown at 850 °C. The appearance of this maximum is explained by inspecting Figure 3 again. With the 2.0 eV laser, we probed a mixture of metallic and semiconducting SWNTs on the samples synthesized at 750 and 950 °C, but majority of metallic SWNTs were on the one synthesized at 850 °C. Therefore,

the contribution of the feature centered at 1540 cm^{-1} is more pronounced on the latter sample.

4. CONCLUSIONS

The diameter of a SWNT obtained by CO disproportionation over Co–Mo catalysts supported on silica gel can be varied by changing the operating temperature. As the temperature is increased, the average SWNT diameter increases. The use of Raman spectroscopy with several excitation lasers is a useful tool to obtain both a complete description of the SWNT diameter distribution and the metallic or semiconducting nature of the nanotubes. Good agreement is obtained between previously published theoretical calculations and the combination of excitation energy and SWNT diameter as inferred from the position of the breathing mode band. At the same time, the analysis of the tangential *G* band including a low-frequency feature, which can be fitted with a Breit–Wigner–Fano line, can be used to distinguish between metallic and semiconducting nanotubes.

Acknowledgments: Financial support from the Department of Energy, Office of Basic Energy Sciences (grant DE-FG03-02ER15345) is greatly acknowledged. JEH acknowledges the Fulbright–CAREC Program for a scholarship.

References and Notes

1. S. Iijima and T. Ichihashi, *Nature* 363, 603 **(1993)**.
2. B. I. Yakobson and R. E. Smalley, *Amer. Sci.* 85, 324 **(1997)**.
3. J. A. Kong, A. M. Cassell, and H. Dai, *Chem. Phys. Lett.* 292, 567 **(1998)**.
4. P. Nikolaev, M. J. Bronikowski, R. K. Bradley, F. Rohmund, D. T. Colbert, K. A. Smith, and R. E. Smalley, *Chem. Phys. Lett.* 313, 91 **(1999)**.
5. B. Kitiyanan, W. E. Alvarez, J. H. Harwell, and D. E. Resasco, *Chem. Phys. Lett.* 317, 497 **(2000)**.
6. A. R. Harutyunyan, B. K. Pradhan, U. J. Kim, G. Chen, and P. C. Eklund, *Nano Lett.* 2, 525 **(2002)**.
7. P. Corio, M. L. A. Temperini, P. S. Santos, J. V. Romero, J. G. Huber, C. A. Luengo, S. D. M. Brown, M. S. Dresselhaus, G. Dresselhaus, M. S. S. Dantas, C. F. Leite, F. Matinaga, J. C. Gonzalez, and M. A. Pimenta, *Chem. Phys. Lett.* 350, 373 **(2001)**.
8. A. Peigney, P. Coquay, E. Flahaut, R. E. Vandenberghe, E. De Grave, and C. Laurent, *J. Phys. Chem. B* 105, 9699 **(2001)**.
9. Y. Li, W. Kim, Y. Zhang, M. Rolandi, D. Wang, and H. Dai, *J. Phys. Chem. B* 105, 11424 **(2001)**.
10. M. Su, Y. Li, B. Maynor, A. Buldum, J. P. Lu, and J. Liu, *J. Phys. Chem. B* 104, 6505 **(2000)**.
11. W. E. Alvarez, F. Pompeo, J. E. Herrera, L. Balzano, and D. E. Resasco, *Chem. Mater.* 14, 1853 **(2002)**.
12. J. E. Herrera, L. Balzano, A. Borgna, W. E. Alvarez, and D. E. Resasco, *J. Catal.* 204, 129 **(2001)**.
13. S. Bandow, S. Asaka, Y. Saito, A. M. Rao, L. Grigorian, E. Richter, and P. C. Eklund, *Phys. Rev. Lett.* 80, 3779 **(1998)**.
14. A. G. Rinzler, J. Liu, H. Dai, P. Nikolaev, C. B. Huffman, F. J. Rodriguez-Macias, P. J. Boul, A. H. Lu, D. Heymann, D. T. Colbert, R. S. Lee, J. E. Fischer, A. M. Rao, P. C. Eklund, and R. E. Smalley, *Appl. Phys. A* 67, 29 **(1998)**.
15. M. Yudasaka, T. Ichihashi, and S. J. Iijima, *Phys. Chem. B* 102, 10201 **(1998)**.
16. M. A. Pimenta, A. Marucci, S. A. Empedocles, M. G. Bawendi, E. B. Hanlon, A. M. Rao, P. C. Eklund, R. E. Smalley, G. Dresselhaus, and M. S. Dresselhaus, *Phys. Rev. B* 58, R16016 **(1998)**.
17. A. M. Rao, E. Richter, S. Bandow, B. Chase, P. C. Eklund, K. A. Williams, S. Fang, K. Subbaswamy, M. Menon, A. Thess, R. E. Smalley, G. Dresselhaus, and M. S. Dresselhaus, *Science* 275, 185 **(1997)**.
18. A. M. Rao, J. Chen, E. Richter, U. Schlecht, P. C. Eklund, R. C. Haddon, U. D. Venkateswaran, Y.-K. Kwon, and D. Tomanek, *Phys. Rev. Lett.* 86, 3895 **(2001)**.
19. R. Saito, M. Fujita, G. Dresselhaus, and M. Dresselhaus, *Appl. Phys. Lett.* 60, 2204 **(1992)**.
20. S. D. M. Brown, A. Jorio, P. Corio, M. S. Dresselhaus, G. Dresselhaus, R. Saito, and K. Kneipp, *Phys. Rev. B* 63, 155414 **(2001)**.
21. E. Richter and K. R. Subbaswamy, *Phys. Rev. Lett.* 79, 2738 **(1997)**.
22. H. Kataura, Y. Kumazawa, Y Maniwa, I. Umezu, S. Suzuki, Y. Ohtsuka, and Y. Achiba, *Synth. Met.* 103, 2555 **(1999)**.
23. P. Corio, S. D. M. Brown, A. Marucci, M. A. Pimenta, K. Kneipp, G. Dresselhaus, and M. S. Dresselhaus, *Phys. Rev. B* 61, 13202 **(2000)**.
24. S. Rols, A. Righi, L. Alvarez, E. Anglaret, R. Almairac, C. Journet, P. Bernier, J. L. Sauvajol, A. M. Benito, W. K. Maser, E. Munoz, M. T. Martinez, G. F. de la Fuente, A. Girard, and J. C. Ameline, *Eur. Phys. J. B* 18, 201 **(2000)**.

Received: 7 May 2002. Revised/Accepted: 21 November 2002.